

Electrochemical Studies of the Inhibition Effect of 4,6-dichloro-2-(methylthio) pyrimidine on the Corrosion of AISI Type 321 Stainless Steel in 1.0 M Hydrochloric Acid

Rola Y. Khaled¹, A.M. Abdel-Gaber^{1, 2, *}, H. M. Holail³

¹Department of Chemistry, Faculty of Science, Beirut Arab University, Lebanon

²Department of Chemistry, Faculty of Science, Alexandria University, Ibrahimia, P.O. Box 426, Alexandria 21321, EGYPT

³Department of Geology, Faculty of Science, Alexandria University, Ibrahimia, P.O. Box 426, Alexandria 21321, EGYPT

*E-mail: a.abdelgaber@bau.edu.lb, ashrafmoustafa@yahoo.com

Received: 7 January 2016 / Accepted: 21 January 2016 / Published: 1 March 2016

The corrosion inhibition effect of 4,6-dichloro-2-(methylthio) pyrimidine (DCMTP) on AISI type 321 stainless steel in 1.0 M hydrochloric acid solution at 30 °C was investigated using potentiodynamic polarization and electrochemical impedance spectroscopy (EIS) technique. Polarization curves showed that DCMTP acts as cathodic type inhibitor. The impedance response indicated that the corrosion process occurs under charge transfer control. Increasing inhibitor concentration led to significant reduction in the corrosion rate of stainless steel with achievable inhibition efficiency of 72% at 8×10^{-4} M DCMTP. Activation parameters E_a , ΔH^* , and ΔS^* were also calculated and discussed.

Keywords: AISI 321, Impedance, Polarization, inhibitor, activation parameters.

1. INTRODUCTION

Stainless steel has a great extent of structural, architectural and engineering applications. It is corrosion-resistant and enduring that make thinner and strong structures possible. The stainless steel used as a construction material in various applications such as piping systems, drilling platforms, heat exchanger equipment's, and chemical, desalination. It offers architects with numerous options of shape and form [1, 2]. The formation of a passive layer on their surface offer high corrosion resistance for these materials. [3].

Scale removal of oil well reservoirs are carried out with (15 % w/v) HCl at temperatures up to 60 °C in order to remove carbonated minerals and iron oxides [4]. Hydrochloric acid founds to be effective in dissolving the plugging of the oil wells, because it forms metal chlorides which dissolve rapidly when compared to phosphates, sulphates and nitrates [5]. On the other hand, hydrochloric acid, brine water, and the water vapour near the sea contain chloride ions that breakdown the protective layers formed at the steel surface causing pitting corrosion [6]. Pitting corrosion is one of the most serious forms of localized corrosion [7]. Because of the aggressiveness of acid solutions, to reduce the corrosion attack on stainless steel, organic compounds are generally used as corrosion inhibitors [8–10].

The aim of this work is to evaluate the corrosion behavior of AISI 321 in 1 M HCl solutions containing different concentrations of 4,6-dichloro-2-(methylthio) pyrimidine (DCMTP) using electrochemical polarization measurements and electrochemical impedance spectroscopy at 30°C.

2. EXPERIMENTAL

AISI type 321 stainless steel (AISI 321) was used as working electrode in the present study. The chemical composition of this AISI 321 is 0.063 wt.% C, 20.65 wt.% Cr, 10.6 wt.% Ni, 1.87 wt.% Mn, 0.9 wt.% Si, 0.53wt.% Mo, 0.483 wt.% Cu, 0.28 wt.% Ti, 0.001 wt.% P, 0.001 wt.% S and the remainder is iron. The AISI 321 specimens used in electrochemical measurements were cut into cylindrical shape of 1 cm² cross sectional area. The AISI 321 specimen was soldered with Cu-wire for electrical connection and was mounted with Teflon to expose surface area of 1 cm² to the electrolyte. The electrodes were abraded with different grades of emery papers, then polished with 0.05-micropolish powder, and rinsed with distilled water and ethanol to remove possible residue of polishing before they were inserted into the test solution.

The detailed description of electrochemical techniques used during this investigation was reported in a previous study [11].

All chemicals used in this work, namely, hydrochloric acid (Analar Normapur, purity 37%), 4,6-dichloro-2-(methylthio) pyrimidine (DCMTP), Figure 1, purchased from Acros, 98% and absolute ethanol (Riedel-de Haen, 99.8%) were reagent grade. Stock solution of 10⁻²M DCMTP was prepared by dissolving the appropriate weight of DCMTP in absolute ethanol. The test solution containing 10% ethanol was prepared by diluting the stock solution and appropriate amount of 4M HCl using ethanol and distilled water.

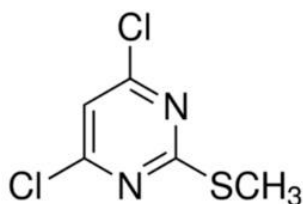


Figure 1. Molecular structure of DCMTP

3. RESULTS AND DISCUSSION

3.1. Potentiodynamic Polarization Data Measurements.

Figure 2 shows the potentiodynamic polarization curves of AISI 321 in 1.0M HCl in the presence and the absence of different concentrations of 4,6-dichloro-2-(methylthio) pyrimidine (DCMTP) at 30 °C. The curves show that addition of DCMTP affect predominantly the cathodic part of the polarization curves indicating that it acts as a cathodic type inhibitor.

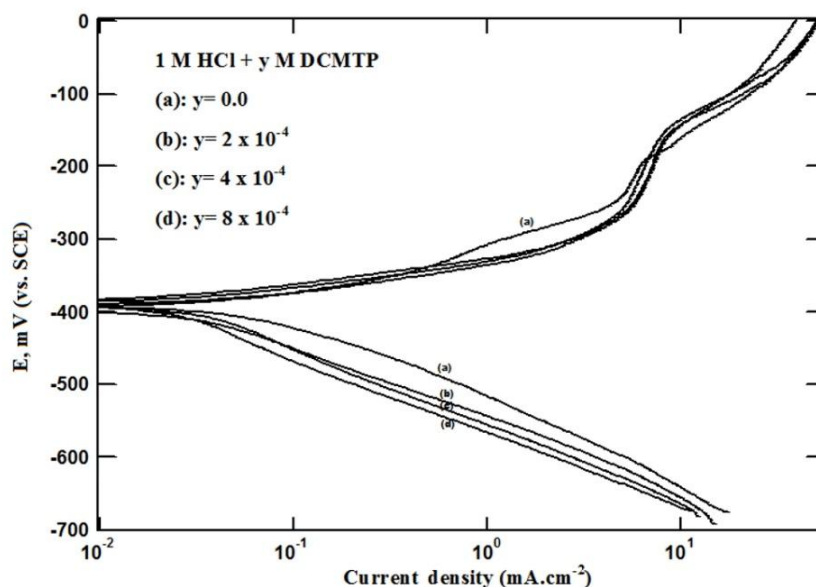


Figure 2. Potentiodynamic polarization curves of AISI 321 in 1.0 M HCl in the presence and the absence of different concentrations of 4,6-dichloro-2-(methylthio) pyrimidine (DCMTP) at 30°C.

The anodic part of the polarization curves of stainless steel in acid chloride media, Figure 1, consist of three distinct regions [12, 13]: (i) the active dissolution region, within the range from -400 to -300 mV (vs. SCE). where active dissolution of iron occurs. This takes place due dissolution of the adsorbed layer of $(\text{CrCl})_{\text{ads}}$, $(\text{NiCl})_{\text{ads}}$ and $(\text{FeCl})_{\text{ads}}$. (ii) the passivity region, that occurs at moderate anodic potential from -300 to -150 mV(vs. SCE), where a thicker oxide film of Fe_2O_3 (s) is formed. The passive layer can be improved because of the formation of Cr_2O_3 (s) and NiO (s) oxides. (iii) the transpassive region that occurs at anodic potential more than -150mV (vs. SCE), the passive layer dissolve.

The electrochemical polarization parameters: corrosion current density (i_{corr}), corrosion potential, E_{corr} ; anodic and cathodic Tafel slopes, β_a , β_c ; obtained from the analysis of polarization curves are given in Table 1.

The percentage of inhibition efficiency (%P) was calculated using the relation:

$$\%P = [(i_{\text{corr}0} - i_{\text{corr}}) / i_{\text{corr}0}] \times 100$$

where $(i_{\text{corr}})_0$ and (i_{corr}) are the corrosion current density in the absence and presence of inhibitor, respectively.

Table 1. The electrochemical polarization parameters of AISI 321 in 1M HCl in the presence and absence of different concentrations of (DCMTP) at 30°C.

[DCMTP] (M)	$-E_{\text{corr}}$ (mV vs. SCE)	β_a	β_c	i_{corr} (mA.cm ⁻²)	%P
		mV.decade ⁻¹			
Blank	391	78	116	0.0837	-
2x10⁻⁴	409	50	93	0.0337	59.7
4x10⁻⁴	399	44	101	0.0276	67.1
8x10⁻⁴	388	41	101	0.0248	70.5

The obtained data indicate that increasing of DCMTP concentration decreases the corrosion current density (i_{corr}) and increases %P. The slight variations in cathodic Tafel slopes (β_c), 90-116 mV/decade, indicates that the rate-determining step for the hydrogen evolution reaction is the discharge of adsorbed hydrogen atoms to form hydrogen molecules. This means that the inhibition of the hydrogen evolution reaction by DCMTP occurs by simple adsorption of cationic form or neutral molecules on the cathodic sites preventing the hydrogen evolution reaction. The corrosion potential E_{corr} is nearly constant in the presence and absence of inhibitor.

3.2. Impedance Data Measurements.

The corrosion of AISI 321 in 1.0 M HCl in the presence and absence of DCMTP was investigated by electrochemical impedance spectroscopy technique (EIS) at 30°C. Nyquist plots in the absence and presence of DCMTP are presented in Figure 3. It is clear that all Nyquist impedance plots show a single capacitive loop of characteristic depressed semicircles indicating that the corrosion process occurs under charge transfer control. The size of the semicircle increases with the increase of DCMTP concentration clarifying that the protection barrier becomes more thickly packed over the surface.

The impedance data of stainless steel in 1.0 M HCl are analyzed in terms of an equivalent circuit model, Figure 4, which includes the solution resistance R_s and constant phase element (CPE) which is placed in parallel to the charge transfer resistance R_{ct} . The CPE consists of the none-ideal double layer capacitance (Q_{dl}) and a constant (n). [14].

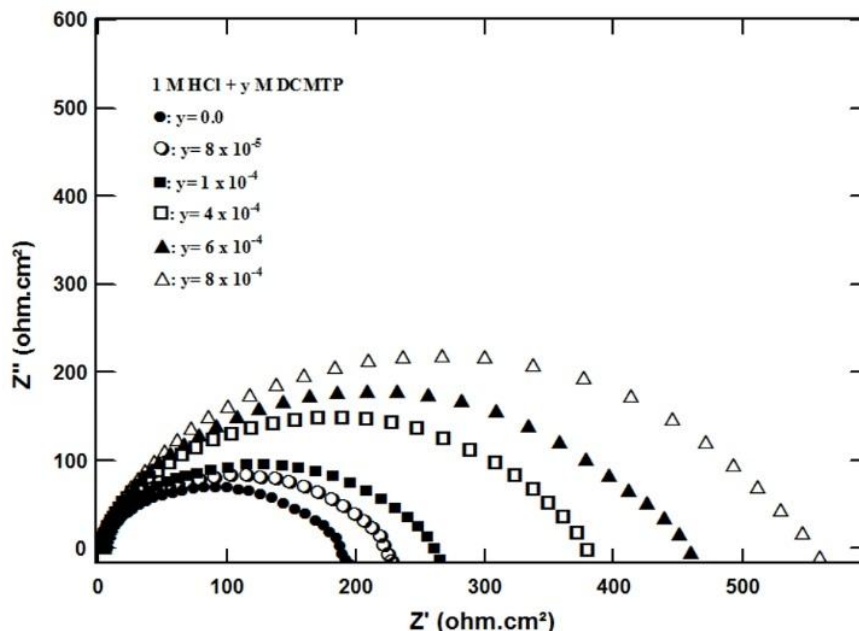


Figure 3. Nyquist Impedance plots for AISI 321 in 1.0 M HCl in the presence and absence of different concentrations of DCMTP mild steel at 30°C.

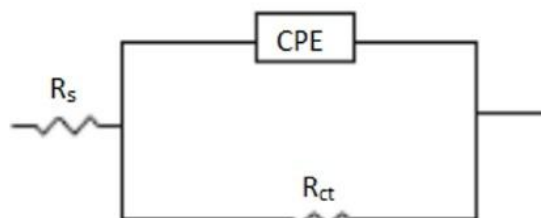


Figure 4. Schematic for the equivalent circuit model

The electrochemical impedance parameter R_{ct} , Q_{dl} and (n) obtained from fitting of experimental impedance spectra of AISI 321 electrode are presented in Table 2. %P can be calculated using the equation:

$$\%P = [(R_{ct} - R_{ct0}) / R_{ct}] \times 100 \tag{1}$$

where R_{ct0} and R_{ct} are the values of the charge transfer resistance ($\Omega \text{ cm}^2$) in the absence and the presence of DCMTP, respectively.

Table 2 indicates that the values of R_{ct} increase with increasing DCMTP concentration denoting increase in the protection efficiency. The values of (n) indicate type of depressed semicircle. It was suggested that the inhibitor adsorbs over the metal surface due to decrease of the values of Q_{dl} with increasing concentration of the inhibitor. The accompanying increase of the thickness of the electrical double layer may be responsible for this decrease in Q_{dl} [15, 16].

Table 2. Electrochemical impedance parameters for AISI 321 in 1.0M HCl containing different concentrations of DCMTP at 30°C.

[DCMTP] mol. L ⁻¹	R _s (Ω.cm ²)	R _{ct} (Ω.cm ²)	Q _{dil} (μF)	n	%P
0	2.03	147	574	0.83	-
8x10 ⁻⁵	1.91	214	565	0.83	31.3
1x10 ⁻⁴	1.91	256	526	0.81	42.5
4x10 ⁻⁴	1.85	367	308	0.86	59.9
6x10 ⁻⁴	2.91	428	276	0.88	65.6
8x10 ⁻⁴	2.52	531	274	0.88	72.3

3.3. Activation Parameters

The potentiodynamic polarization curves for dissolution of AISI 321 in 1.0 M HCl in the presence of 8x10⁻⁴ M DCMTP at different temperatures are shown in Figure 5. The figure indicates that increasing temperature enhances both cathodic and anodic parts of the curves and consequently the corrosion rate.

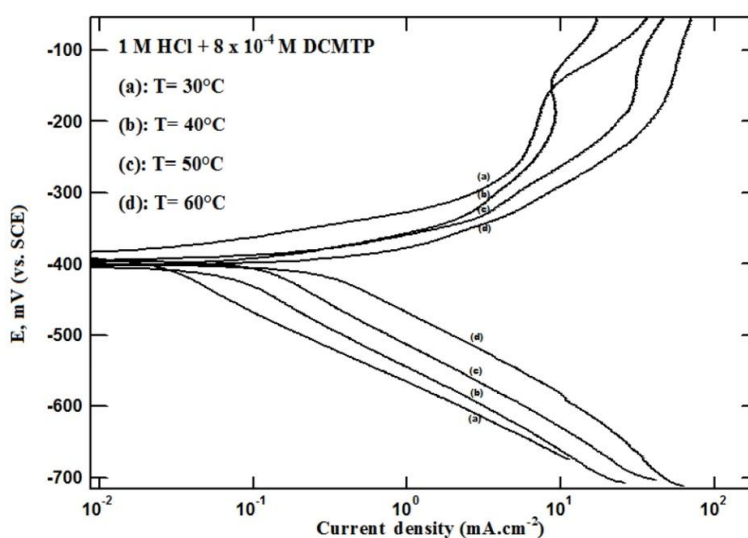


Figure 5. Potentiodynamic polarization curves for dissolution of AISI 321 in 1.0 M HCl in the presence of 8x10⁻⁴ M DCMTP at different temperatures

The electrochemical polarization parameters for AISI 321 in 1.0 M HCl in the presence and the absence of different concentrations of (DCMTP) at different temperatures are shown in Table 3. The data indicate that, at any given temperature, the corrosion current density in the absence of DCMTP is higher than that in its presence.

The apparent activation energy, E_a; the apparent enthalpy of activation, ΔH^{*}; the apparent entropy of activation, ΔS^{*} for dissolution of AISI 321 in the absence and presence of 8x10⁻⁴ M DCMTP were obtained using Arrhenius and the transition state equations [17] from linear square fit of

$\ln(i_{\text{corr}})$ and $\ln(i_{\text{corr}}/T)$ data vs. $(1/T)$. The calculated values of E_a and ΔH^* and ΔS^* are presented in Table 4.

Table 3. The electrochemical polarization parameters for AISI 321 in 1.0 M HCl in the presence and absence of different concentrations of (DCMTP) at different temperatures.

	Temperature (°C)	E_{corr} , mV	β_a $-\beta_c$		i_{corr} , mA/cm ²
			mV/decade		
1.0 M HCl	30	391	78	116	0.0837
	40	388	78	108	0.103
	50	378	68	122	0.218
	60	398	82	109	0.375
1.0 M HCl + 8×10^{-4} M DCMTP	30	388	41	101	0.025
	40	429	65	109	0.086
	50	463	138	112	0.351
	60	347	131	113	0.637

Table 4. The activation parameters of AISI 321 in 1.0 M HCl in the absence and presence of 8×10^{-4} M DCMTP.

[DCMTP]	E_a (Kj.mol ⁻¹)	ΔH^* (kJ.mol ⁻¹)	$-\Delta S^*$ (J. mol ⁻¹ k ⁻¹)
-	43.78	41.15	1171
8×10^{-4}	93.80	91.15	1327

Comparing apparent activation energy (E_a) gives several information about the mechanism of the inhibiting action. The higher values of E_a and ΔH^* in the presence of DCMTP suggest to its protective effect. The data indicate that the formation of the activated complex is endothermic process because ΔH^* have positive values. The increase of the activation energy in the presence of DCMTP could be attributed to the adsorption of the cationic form of DCMTP on steel surface. In addition, the negative values of ΔS^* indicate that the transfer of reactants to the activated complex is accompanied by decrease in disordering [18-19].

3.3. Adsorption Considerations

The corrosion inhibition of most organic inhibitors may be due to adsorption at the metal/solution interface [20]. Fitting of degree of surface coverage obtained from impedance measurements ($\theta = \%P/100$) to Langmuir, Florry- Huggins isotherms, and Kinetic – thermodynamic model were done. The details of these isotherms and model were discussed elsewhere [14].

The parameters obtained from these isotherms and model having R^2 values of 0.99, which describe the goodness of fit, are depicted in table 5. The tabulated data indicate that DCMTP does not

fit Langmuir adsorption isotherm indicating that the inhibitor is not ideally adsorbed over the metal surface.

Table 5. Linear fitting adsorption parameters of 8×10^{-4} M DCMTP over AISI 321 in 1.0 M HCl according to all mentioned models at 30 °C.

Kinetic- thermodynamic Model		Florry-Huggins	
K	1/y	K	x
4466	1.49	3816	1.88

The parameters obtained from application of Florry- Huggins isotherms, and Kinetic – thermodynamic model indicates that the size parameter x, number of absorbed water molecules substituted by a given DCMTP molecule and 1/y, the number of active sites occupied by a single DCMTP molecule are greater than unity indicating that DCMTP is bulky.

The binding constant (equilibrium constant of adsorption), K is related to the standard free energy of adsorption (ΔG_{ads}), with the following equation [21].

$$K_{ads} = 1/55.5 e^{(-\Delta G_{ads}/RT)}$$

Where R is the molar gas constant, T is the absolute temperature in Kelvin and 55.5 is the concentration of water in solution expressed in molar. The stability and spontaneity of the adsorption process of DCMTP on AISI 321 surface in acidic solutions are reflected by the negative values of the ΔG_{ads} . Physisorption mechanism is consistent with values of ΔG_{ads} up to $-20 \text{ kJ}\cdot\text{mol}^{-1}$, chemisorption mechanism is associated with ΔG_{ads} around $-40 \text{ kJ}\cdot\text{mol}^{-1}$ or higher [21-23]. The values of ΔG_{ads} were calculated from the kinetic-thermodynamics model data and Florry-Huggins isotherm and found to be $-31.29 \text{ kJ}\cdot\text{mol}^{-1}$ and $-30.9 \text{ kJ}\cdot\text{mol}^{-1}$, respectively. These values indicate that the adsorption of DCMTP molecules over metal surface is not physisorption or chemisorption but comprehensive adsorption mechanism (physicochemical adsorption).

4. CONCLUSIONS

There has been very little research reported for studying the corrosion of AISI 321 in acidic solution [23, 24]. Hydrochloric acid attacks AISI 321 since the acid readily destroy its passivity. 4,6-dichloro-2-(methylthio) pyrimidine (DCMTP) shows reasonable inhibitive effect for the acidic corrosion of AISI 321 that is widely used in chemical processing equipment, Jet Engine Parts, Welded Equipment, etc. DCMTP acts as a cathodic type inhibitor for AISI 321 in 1.0 M HCl. The inhibitive action of DCMTP is attributed to the adsorption of the inhibitor over the metal surface. The adsorption of DCMTP molecules on metal surface is suggested to be physicochemical adsorption.

References

1. B.N. Mordyuk, G.I. Prokopenko, M.A.Vasylyev, M.O. Iefimov, *Mater. Sci. Eng., A* 458 (2007) 253–261

2. Chuan-bo Zheng, L. Cai, Zhu-jun Tang, Xiao-lan Shen, *Surf Coat Technol*, 287 (2016)153–159
1. A. Pardo, M.C. Merino, E. Coy, F.Viejo, R. Arrabal and E. Matykina, *Corros. Sci.*, 50 (2008)780–794.
2. A.L.d.Q. Baddini, S.P. Cardoso, E. Hollauer and J.A.d.C.P. Gomes, *Electrochim. Acta*, 53 (2007) 434–446.
3. P. Rajeev, A.O. Surendranathan and Ch.S.N. Murthy; *J. Mater. Environ. Sci.*, 3 (2012) 856-869.
4. G.T. Burstein, C. Liu, R.M. Souto and S.P. Vines, *Corros. Eng. Sci. Technol.*, 39 (2004) 25–30.
5. M.G. Fontana and N.D Greene, *Corrosion Engineering*, 3rd edition, McGraw-Hill, New York, 1987.
6. A.S. Fouda, M. Abdallah, S.M Al-Ashrey and A.A. Abdel-Fattah, *Desalination*, 250 (2010) 538–543.
7. R. Fuchs-Godec, *Electrochim. Acta*, 54 (2009) 2171–2179.
8. N. Caliskan and E. Akbas, *Mater. Chem. Phys.*, 126 (2011) 983–988.
9. B. Cai, Y. Liu, X Tian, F. Wang, H Li, R Ji, , *Corros. Sci.*, 52 (2010) 3235–3242
10. M Scendo, J Trela, *Int. J. Electrochem. Sci.*, 8 (2013) 9201-9221
11. Kh. M. Hijazi, A. M. Abdel-Gaber, G. O. Younes, *Int. J. Electrochem. Sci.*, 10 (2015) 4366 - 4380
12. S. Gudić, L. Vrsalović, M. Kliškić, I. Jerković, A. Radonić, M. Zekić, *Int. J. Electrochem. Sci.*, 11 (2016) 998 – 1011
13. M. Benabdellah, R. Touzani, A. Dafali, B. Hammouti, S. El Kadiri, *Mater. Lett.*, 61 (2007) 1197–1204.
14. A. Ghanbari, M.M. Attar, M. Mahdavian, *Mater Chem. Phys.*, 124 (2010)1205–1209.
15. A.M. Abdel-Gaber, H.H. Abdel-Rahman, A.M. Ahmed and M.H. Fathalla, *Anti-Corros Method and Mater*, 53 (2006) 218 – 223.
16. O.R. Khalifa and S.M. Abdallah, *Portugaliae Electrochim. Acta*, 29 (2011)47-56.
17. G. Cristofari, M. Znini, L. Majidi, A. Bouyanzer, S.S. Al-Deyab, J. Paolini, B. Hammouti and J. Costa, *Int. J. Electrochem. Sci.*, 6 (2011) 6699 – 6717.
18. I.B. Obot, *Portugaliae Electrochim. Acta*, 27 (2009) 539-553.
19. N. O. Eddy and E. E. Ebenso, *Afr. J. Pure Appl. Chem.*, 2 (2008) 46-54.
20. N.J.N. Nnaji, N. O. Obi-Egbedi and J.U. Ani , *J. Sci. and Ind. Studies*, 9 (2011) 26-32
21. H. Ashassi-Sorkhabi, B. Shaabani, B. Aligholipour and D. Seifzadeh, *Appl. Surf. Sci.*, 252(2006)4039-4047.
22. A. S. Fouda, and H. El-Dafrawy *Int. J. Electrochem. Sci.*, 2 (2007) 721-733.
23. Y. L. Huang, C. N. Cao, M. Lu, and H. C. Lin, *Corrosion*: 49(1993) 644-649